RESEARCH ARTICLE

The spatial-temporal variations and influencing factors of city's PM10, SO_2, NO_2, and API

Xiuhong Gao*

Hebi Automotive Engineering Professional College, Hebi 456200, Henan, China

Received: August 11, 2023; **accepted:** October 2, 2023.

With the development of urban economy and the improvement of people's living standard, environmental problems have become the focus of people's attention. Among them, air pollution not only restricts the speed of economic development, but also affects the health level of the people. This study used the global spatial autocorrelation method, spatial descriptive statistics, and other index methods to explore the changing trend of spatial and temporal characteristics and influencing factors of urban air pollutants. The results showed that the air pollutions of PM10, SO_2, NO_2, and air pollution index (API) were mainly concentrated in spring and winter, and there was an obvious "weekend effect." Pollutants had a certain spatial dependence, and the pollution center gradually shrank from the northwest to the northeast of China. Population density and urban economic level had a negative relationship with API and main pollutants, while economic level and API had positive correlation. The results of this study provided references for scientifically coping with the characteristics of seasonal pollution transformation and strengthened the joint prevention and control mechanism of air pollution by exploring the change rules and influencing factors of air pollutants, so as to form a green and coordinated development pattern.

Keywords: urban spatial pollution index; spatial-temporal change law; impact factor evaluation; air pollution index.

***Corresponding author:** Xiuhong Gao, Hebi Automotive Engineering Professional College, Hebi 456200, Henan, China. Email: glxh1220@126.com.

Introduction

The continuous development of urbanization has led to rapid economic growth and promoted the process of industrialization, and the quality of people's life has been continuously improved under this background. In addition, the increase in per capita disposable income makes people's demand for cars gradually rise. As a result, the number of cars in the city shows a rising trend. However, vehicle exhaust emissions contain more pollutants that harm urban air quality, including sulfur dioxide (SO_2), nitrogen dioxide (NO_2), and inhalable particulate matter (PM10). The increasing content of these air pollutants makes the environmental health of the city face a greater challenge. In addition, environmental pollution is also one of the realistic constraints in the decisive stage of building a moderately prosperous society in an all-round way [1-3]. Therefore, affected by factors such as the surge of population and the improvement of economic development level, the problem of air pollution in Chinese cities has become increasingly serious, and the negative environmental effects caused by it are relatively obvious [4, 5].

Studies related to the spatial and temporal distribution of air pollution mainly use multidisciplinary methods such as mathematics, geography, meteorology, *etc*. to carefully analyze the concentration value or comprehensive index

of pollutants in the whole region or local region on different time scales to obtain its time change trend and spatial distribution characteristics in the corresponding period. The research results of air pollution provide a scientific and reliable basis for the formulation of air pollution control measures, which has attracted more scholars' attention. Geng *et al*. developed a near-real-time air pollution database to better understand the spatial and temporal distribution of air pollution. The database combined information from multiple data sources such as ground observations, satellite aerosol optical depth, meteorological fields, and land use data. The database constructed could track the daily changes of PM in real time, which was more convenient for the study of the spatial and temporal distribution of air pollution [6]. Gui *et al*. took dust pollutants as the research object and used Euler-Lagrange model to study the motion law and space-time distribution of dust. The results showed that the wind curtain jet changed with the development of time and space and had a significant impact on the surrounding flow field. This study had effectively discussed the spatial and temporal distribution law of dust air pollutants [7]. Further, Kerimray *et al*. investigated the influence of meteorological conditions on air pollutant diffusion in highly polluted industrial and mining cities by using inverse distance weighted interpolation method. In addition, by combining wind speed, wind direction and precipitation data, the pollution process, temporal distribution, spatial distribution, and meteorological conditions of heavy air pollution in the studied area were discussed, which provided new insights into mitigating air pollution in industrial cities [8]. Moreover, Ma *et al*. found that the air pollution model based on the traditional land regression model had the limitation of complex operation and proposed a LUR modeling and pollution mapping software called PyLUR, which included potential predictor variable generation, regression modeling, model verification module, and prediction mapping, and could efficiently generate pollutant concentration maps [9]. Liu *et al*. analyzed the temporal and spatial distribution of ozone and its impact on human health by using a variety of cross-scientific methods. The results showed that the spatial distribution of ozone was mainly in the northwest to southeast direction, showing the characteristics of spatial autocorrelation with the time characteristics of "high in summer and winter, low in spring and autumn" [10]. The study of air pollution influencing factors focuses on the influence of air pollution on air quality in time, space, and region. Many studies have explored the relationship between air pollution and environmental factors from the aspects of nature and social economy to provide evidence for air pollution prevention and control. From the perspective of environmental risk, Du *et al*. adopted spatial statistical method and geographical regression weighting model to analyze the spatial characteristics of risks and assess the key areas where risks occurred respectively [11]. Based on China's annual atmospheric monitoring data, Bai *et al*. used ArcGIS and principal component analysis to monitor the atmospheric environment data of a certain province and found that heavy coal burning and vehicle emissions in winter led to severe regional pollution. The pollutants' time distribution was winter greater than summer, while the spatial distribution showed a decreasing trend from northwest to southeast [12]. In addition, Yang *et al*. studied the relationship between air quality, air pollutant characteristics, and meteorological factors in Beijing and Tianjin, China and found that most pollutants were positively correlated with temperature, while ozone was generally only positively correlated with temperature in autumn, and NO_2 was negatively correlated with temperature in autumn. Among the pollutants, PM10, PM2.5, and CO had greater impacts on air quality index (AQI) [13]. To explore the influencing factors of air pollutants, Wang *et al*. adopted nonlinear Grann causality test technology to identify the spatial correlation of air pollution. In addition, based on relational data, a secondary assignment program was applied to discuss the factors affecting the spatial correlation of haze pollution in North China. Regression analysis showed that geographical

distance matrix, economic development level, and environmental regulation level could affect urban haze pollution [14]. A roadside monitoring experiment to explore the relationship between urban traffic and air pollution was conducted by Zhang *et al*, which studied the rule and key influencing factors of air pollutants emitted by urban traffic. The results showed that the mass concentration of air pollutants in various districts of the city was mainly affected by motor vehicle emissions. and illumination, wind speed and direction could significantly affect the diffusion of air pollutants [15].

The increase in population density, competition for energy consumption and the increase in the number of motor vehicles are particularly evident in large cities and have caused great changes in the types of air pollution sources and the concentration levels of pollutants. Nitrogen oxides and hydrocarbons are closely related to reduced visibility and frequent haze weather [16], while PM10, SO_2, NO_2, and other pollutants will cause damage to human tissues and organs and increase the possibility of viral infection [17]. The study on the spatial-temporal evolution characteristics of urban air pollution can provide theoretical support for the development of urban air pollution prevention and control work. It can also provide a scientific basis for the formulation of further air pollution prevention and control strategies. Although many studies have paid more attention to the spatial and temporal distribution and influencing factors of air pollution, there are still limitations such as the selection of air pollutants was not rich enough, the index of measuring air pollutants had strong subjectivity, and the research period needed to be further extended. Therefore, this study adopts global spatial autocorrelation method, spatial descriptive statistics, and other index methods to explore the changing trend and influencing factors of spatial and temporal characteristics of urban air pollutants. The results of this study could be helpful in formulating appropriate improvement strategies to further accelerate economic development and improve people's life happiness index.

Materials and methods

Data resource and processing

The data of air pollution index (API) and major pollutants from 329 prefecture level and above cities in China from 2020 to 2022 were included in this study. The hourly monitoring data of all APIs were obtained from the China Environmental Monitoring Station, which were organized and summarized on a small to large time scale. The geographic information system software, ArcGis 10.8 (Esri, Redlands, California, USA) was employed to statistically organize the changes in API values for 2020 and 2021 to understand the spatial distribution and movement of API and major air pollutants over the course of a year. A total of 9 environmental air quality monitoring stations were set up by The Environmental Protection Bureau of Nanchang City (Nanchang, Jiangxi, China). The daily hourly air quality data from those 9 monitoring stations in 2017 was retrieved from the website of the Environmental Protection Department of Jiangxi, China. The single indicator data including hourly data from the Chinese New Year's Eve, the first day of the lunar new year, and the second solstice (spring equinox, summer solstice, autumn equinox, and winter solstice) of Nanchang City from 2016 to 2022, as well as daily hourly pollution and meteorological data including temperature, humidity, and wind speed from April, July, October 2017, and January 2018 were obtained from the China Air Quality Online Monitoring and Analysis Platform. The daily API, quality level, and primary pollutant data of Nanchang City from 2016 to 2022 were obtained from the Data Center of the Ministry of Environmental Protection of China. The meteorological data used in the backward trajectory model was from Global Data Assimilation System (GDAS) (National Centers for Environmental Information, Asheville, North Carolina, USA).

To explore the socio-economic factors of urban air pollution, the constructed model was applied to analyze the data and explain the variables. Subsequently, an assessment model of

environmental impact was generated by using the explanatory variables in the STIRPAT theoretical model. The control variables of the model were the total commonly used population, regional per capita GDP, nighttime lighting value, and urban technological level, which were incorporated into the formula model for regression analysis.

Spatial and temporal distribution mode of urban air pollutants

API implements dimensionless number transformation for air quality evaluation in the form of hierarchical representation, which can effectively express the content and concentration of common air pollutants in numerical form as shown in equation 1 [18].

$$I_i = \frac{C_i - C_{i,j}}{C_{i,j+1} - Ci,j}\left(I_{i,j+1} - I_{i,j}\right) + I_{i,j}\left(j = 1,2,...6, i = 1,2,...,n\right) \quad (1)$$

where $I_i, I_{i,j}$ was the i-th pollutant and its sub-index at the turning point of $j+1$. C_i was the concentration value of pollutant i -th unit content. $C_{i,j+1}$ was the concentration limit of pollutant i at the turning point $j+1$. There was a certain degree of correlation between things, and things that were close to each other having a higher degree of correlation. Accordingly, there might also be a certain correlation between air pollution in different regions [19]. Therefore, the global spatial autocorrelation method (Moran's I index) was introduced to quantitatively describe the spatial similarity and correlation of API as shown in equation 2.

$$I = \frac{\sum_{i=1}^{n}\sum_{j=1,j\neq i}^{n} w_{ij}\left(x_i - \bar{x}\right)\left(x_j - \bar{x}\right)}{\sum_{i=1}^{n}\left(x_i - \bar{x}\right)\sum_{i=1}^{n}\sum_{j=1}^{n} w_{ij}} \quad (2)$$

where w_{ij} was the spatial weight matrix of space unit i and research unit j within the research scope. x_i was the observed value of unit i. $\bar{x}$ was the average of the observed values of each unit. n was the number of subregions of the study area. The range of Moran's I index was between -1 and 1. AQI spatial similarity increased when Moran's I index approached 1. When Moran's I index was close to 0, the spatial distribution of AQI was random. As Moran's I index tended to -1, AQI became more spatially different. When other conditions were the same, the difference of Moran's I index was related to the difference of spatial weighting matrix. While considering the spillover effect of air pollution, the spatial change characteristics of data sampling points were explored, and a regression model was built to analyze the regional diffusion degree and influencing factors of air pollution in terms of geographical characteristics to grasp the spatial evolution law of pollutants more comprehensively. Its calculation equation was shown below.

$$\begin{aligned} LnAPI_i = {} & a\left(\mu_i, v_i\right) + \beta_1\left(\mu_i, v_i\right) LnGDP_i + \beta_2\left(\mu_i, v_i\right) LnDensity_i \\ & + \beta_3\left(\mu_i, v_i\right) LnInno_i + \sum_k \beta_k\left(\mu_i, v_i\right) x_{ik} + e_i \end{aligned} \quad (3)$$

where $\left(\mu_i, v_i\right)$ was the longitude and latitude coordinates of the city i. $a\left(\mu_i, v_i\right)$ was the constant term of city i. $\beta_1, \beta_2, \beta_3$ denoted undetermined values for the assessment of socio-economic levels, population constants, and urban urbanization levels. $\beta_k\left(\mu_i, v_i\right)$ was the city i estimates the parameter value of variable k. x_{ik} was the k-th explanatory variable in city i. e_i was the residual term.

Construction of urban pollution influencing factors analysis model

The environmental Kuznets curve examines the relationship between per capita curve and environmental pollution. With the development of economy, environmental pollution continues to increase so that, when the node value is crossed, economic growth will reduce the generation of environmental pollution [20]. However, with the increase of population and the improvement of scientific and technological level, it is difficult to judge the air pollution problem in environmental problems and the change trend of the increase and decrease of air pollution indicators [21]. Therefore, based on the

STIRPAT model, this study proposed a new benchmark model as equation 4.

$$\begin{cases} \ln(Pollution_{it}) = \alpha_0 + \alpha_1 \ln pop_{it} + \alpha_2 (\ln pop_{it})^2 + \alpha_3 \ln gdp_{it} + \alpha_4 (\ln pop_{it})^2 + \\ \qquad \alpha_5 (\ln pop_{it})^3 + \alpha_6 \ln tec_{it} + \alpha_7 X_{it} + \mu_i + \lambda_t + \varepsilon_{it} \\ \ln(Pollution_{it}) = \alpha_0 + \alpha_1 \ln pop_{it} + \alpha_2 \ln gdp_{it} + \alpha 3 \ln tec_{it} \\ \qquad + \alpha_4 \ln pop_{it}^{*} + \ln gdp_{it} + \alpha_5 X_{it} + \mu_i + \lambda_t + \varepsilon_{it} \end{cases} \quad (4)$$

where $Pollution$ was the environmental pollution index. α_0 was the invariant characteristics of the city during the sample observation period. pop denoted the total population of the city at the end of the year. gdp denoted the GDP per capita measured at prices for that year. tec denoted the level of technology. μ_i indicated urban fixed effects. λ_t represented a time-fixed effect. ε_{it} was a random disturbance term. i indicated the city. t indicated the year. X was a set of related control variables. $\sec$ denoted the industrial structure. Meanwhile, gdp^2 and pop^2 were introduced to further explore whether there was an "N" type relationship between economic growth and air pollution environment. In addition, the least squares model and ArcGis software were combined to further analyze the correlation among factors by using equation 5.

$$\begin{aligned} &LnI = Lna + bLnP + cLna + dLnT + Lne \\ &LnAPI = a + \beta_1 LnGDP + \beta_2 LnDensity + \beta_3 LnInno + \beta_4 Ln\sec \\ &\qquad + \beta_5 LnCons + \beta_6 LnFC + \beta_7 LnPM_{10} + e \end{aligned} \quad (5)$$

where *I*, *P*, *A*, *T* represented the environmental factors that affected the degree of air pollution, the population macro factors, the accumulation of social wealth, and the level of technology that affected the level of urbanization. a was a constant value. *b*, *c*, *d* were the coefficients to be estimated. $Cons$ denoted the built-up area of the city. FC was the urban transport conditions.

The least square regression model takes the spatial independence of multiple variables as the basic assumption. However, due to the action of natural factors such as air circulation, air pollution would spread to the surrounding area. In other words, the degree of local air pollution was not only related to local economic conditions, but also related to the surrounding environment. Therefore, in the process of establishing the spatial econometrics model, the influence of spatial lag must be considered. Since the spatial delay model could consider the spatial dependence of air pollution, a spatial lag model was selected for numerical simulation of the spatial spillover effect of air pollution with its specific function form shown below.

$$\begin{aligned} LnAPI = {} & a + \rho WLnAPI + \beta_1 LnGDP + \beta_2 LnDensity + \beta_3 LnInno + \beta_4 Ln\sec \\ & + \beta_5 LnCons + \beta_6 LnFC + \beta_7 LnPM_{10} + e \end{aligned} \quad (6)$$

where *W* was the spatial weight matrix of *n*×*n*. *n* was the number of cities. $WLnAPI$ was the spatial lag term of the dependent variable. ρ was the autoregressive coefficient in the spatial lag model. If ρ was significant, the local air pollution was affected by air pollution in the surrounding area, while ρ > 0 indicated that an increase in ambient air pollution would lead to an increase in local air pollution. Ordinary least squares regression ignores spatial heterogeneity. To improve this limitation, Geographically Weighted Regression (GWR) model was proposed in this study to consider the effect of spatial heterogeneity. Its specific function expression was shown in equation 7.

$$\begin{aligned} LnAPI_i = {} & a(\mu_i, v_i) + \beta_1(\mu_i, v_i) LnGDP_i + \beta_2(\mu_i, v_i) LnDensity_i \\ & + \beta_3(\mu_i, v_i) LnInno_i + \sum_k \beta_k(\mu_i, v_i) x_{ik} + e_i \end{aligned} \quad (7)$$

where (μ_i, v_i) represented the longitude and latitude coordinates of the city i. $a(\mu_i, v_i)$ was a constant term representing a city i. $\beta_1, \beta_2, \beta_3$ indicated social affluence, demographic factors, and level of technology. $\beta_k(\mu_i, v_i)$ denoted the parameter to be estimated for explanatory variable k of city i. x_{ik} was the k -th explanatory variable representing the i city. e_i represented the residual term of city i. In this study, Gaussian function was selected for regression of spatial weight function, and its specific expression was shown in equation 8.

$$W_i = \phi(d_i / \delta\theta) \quad (8)$$

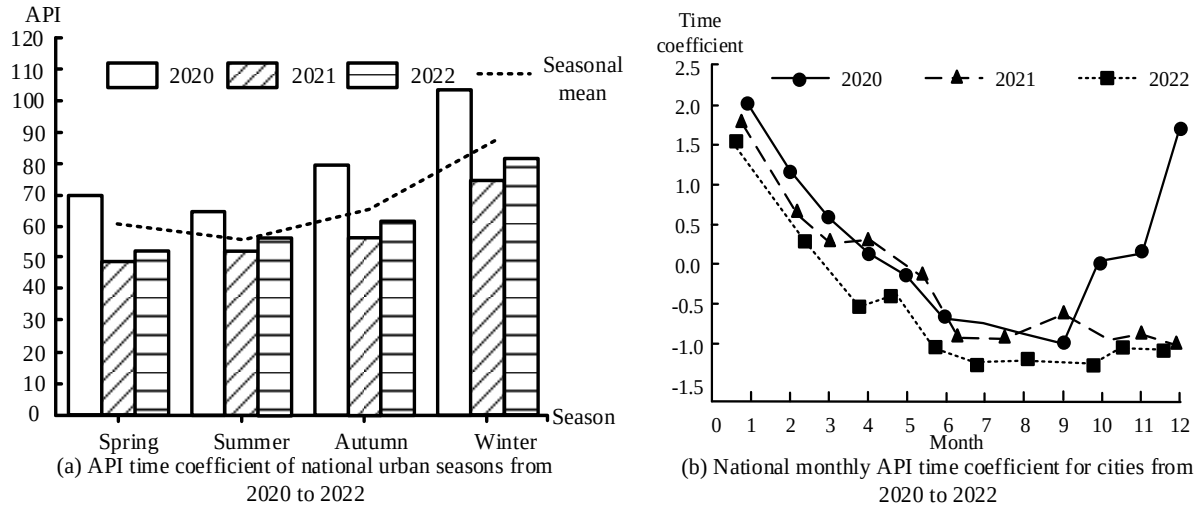

(a) API time coefficient of national urban seasons from 2020 to 2022

(b) National monthly API time coefficient for cities from 2020 to 2022

Figure 1. Distribution of API time coefficients for cities in China by quarter and month from 2020 to 2022.

where ϕ represented the standard normal density function. δ represented the standard deviation of the distance vector d_i. θ was the attenuation coefficient.

Results and discussion

Space-time characteristics of PM10, SO_2, NO_2, and API

The maximum and minimum urban API values of 104.2 and 67 were shown in winter and summer of 2020, respectively. Compared with 2020, the API values in fall and winter of 2021 decrease by 45% and 16.67%, respectively. The values of the API index in 2022 had increased to varying degrees with the winter value rising by 7. The highest mean value in winter was 89.63 while the lowest in summer was 52.43 (Figure 1a). The monthly mean value of API showed a trend of first decreasing and then increasing with September as the turning point of value change for 2020, while the mid to late July and October for 2021 and 2022, respectively (Figure 1b). Influenced by the special epidemic in the second half of 2021 and the changes in living habits, vegetation, and precipitation brought by seasonal changes, the difference between the numerical changes in 2022 and 2021 was small, which changed the concentration of air pollution to a certain extent. To further understand the change characteristics of API and major pollutants, PM10, SO_2, NO_2, and API were analyzed, which all demonstrated a "V" shape with the peaks all appeared in January-March and October-December, indicating serious pollution in winter (Figure 2). The concentrations of PM10 and API values were mostly above 50 μg/m³. The maximum value of SO_2 occurred between 8 am and 11 am with the concentrations of SO_2 and NO_2 were lower than 50 μg/m³, while the concentrations of PM10 and API showed an upward trend after 2 am and 8 PM, indicating that the increase in travel volume after evening aggravated the level of air pollution and increased the number of inhalable particles (Figure 2b). Figures 2c and 2d showed that there was an obvious "weekend effect" in the moment level of pollutants. To grasp the spatial distribution and movement status of API and major air pollutants in one year, the ArcGis tool was used to statistically organize the changes of API values in 2020 and 2021 (Figure 3). The results showed that most parts of the country were in a good level of air quality in 2021 compared to 2020. The pollution level in the southwest part of the Shandong Peninsula urban agglomeration and some parts of Hebei Province had improved, and the pollution level in Kashgar

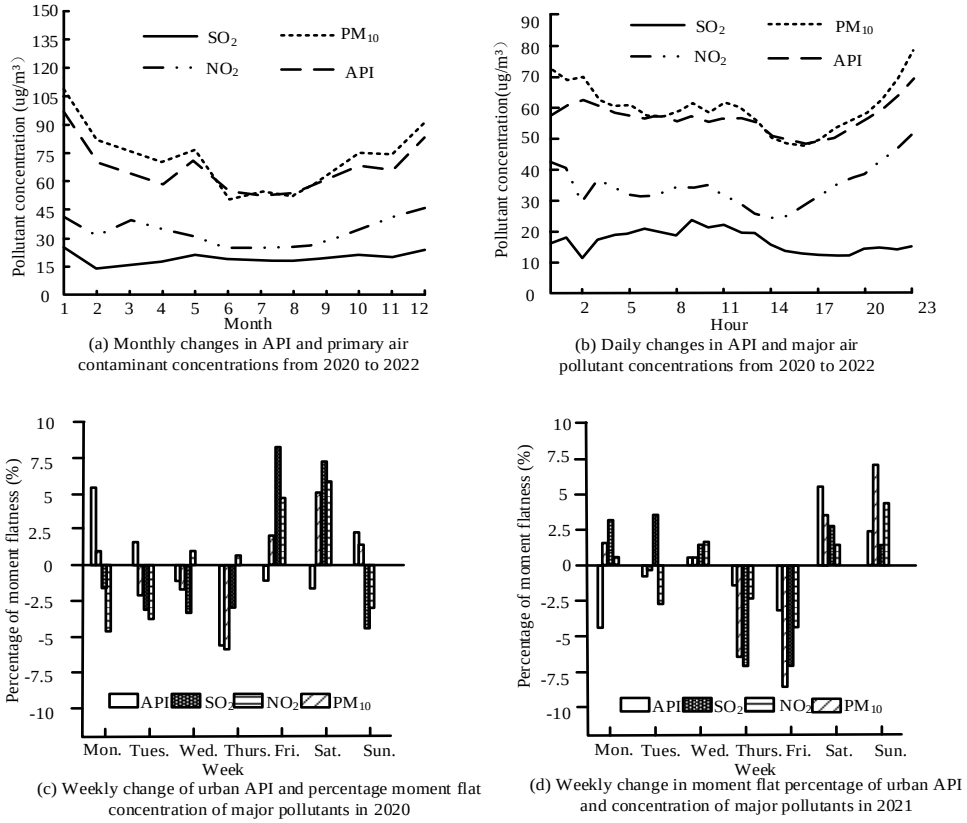

Figure 2. Change characteristics of API and concentration of major pollutants from 2020 to 2022.

had decreased by 22.2%, while the pollution level in western Tibet had increased. In general, the pollution centers in central and eastern China gradually shrank from northwest to northeast, while the air pollution in western China was always in western Xinjiang area (Figure 3a, 3b, 3c). The Moran's I of API was basically above 0.55, and its monthly average had a certain spatial agglomeration characterization (Figure 3d). The index values in January, June, and December of each year were higher, indicating that the concentration degree of air pollution was relatively obvious. The daily variation characteristics of air pollution in the Nanchang city, Jiangxi province, China were demonstrated in Figure 4. The daily variation characteristics of API, PM10, SO_2, and NO_2 all showed a "W" shape trend with the two peaks appearing at 9:00-11:00 and 20:00-22:00, respectively. The daily variation of air pollution in the city was dominated by the traffic exhaust pollution caused by the rush hours. In addition, as the number of cars increased, the proportion of NO_2 emitted by the automobile in the total emissions increased year by year. The monthly change characteristics of API, PM10, SO_2, and NO_2 in 2022 were demonstrated in Figure 5 with all showing a "V" shape and the two peaks appearing from January to March and from October to December, respectively, indicating that the pollution was more serious in winter. Since March, the air had gradually improved with the best air quality in July. However, from September to January, air pollution gradually increased and peaked. The target city is a typical subtropical monsoon climate zone with northerly winds and dirty air in winter. In addition, the city has less rainfall in winter, which is not conducive to the spread of pollutants. The high temperature and rainfall in summer are conducive to the removal of pollutants.

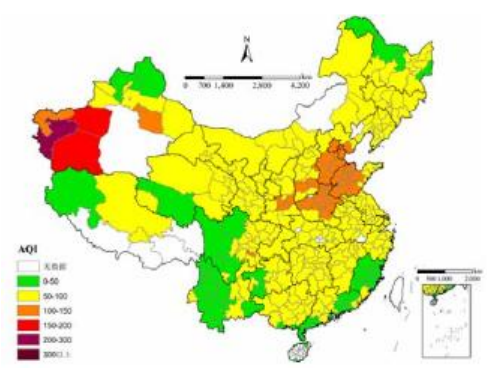

(a) Changes in API values in 2020

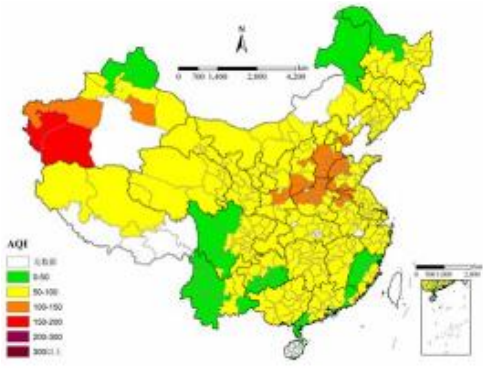

(b) Changes in API values in 2021

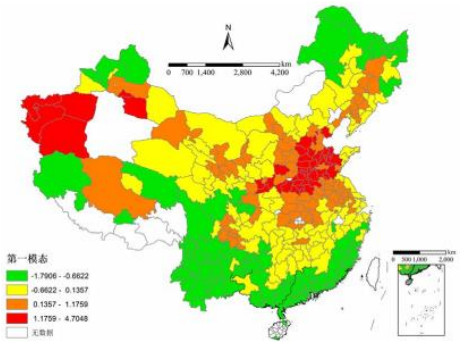

(c) First mode spatial distribution of API monthly mean concentration value EOF in 2020-2021

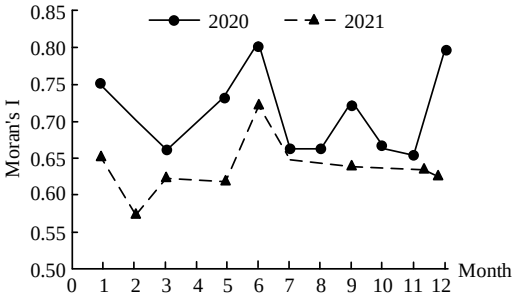

(d) Moran's I trend chart of the national urban API monthly mean value from 2020 to 2021

Figure 3. Distribution of API values and trend of Moran's I index in 2021-2022.

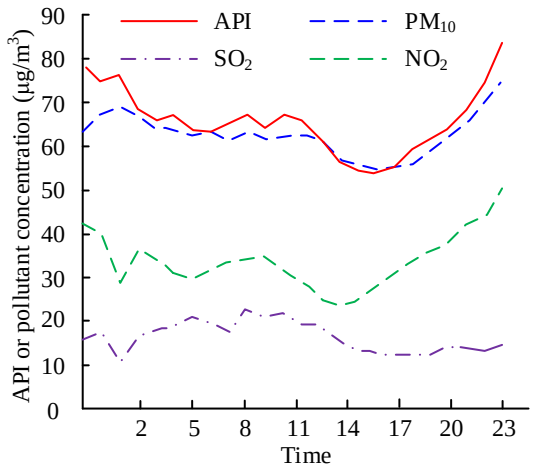

Figure 4. Daily variation characteristics of air pollution in the city.

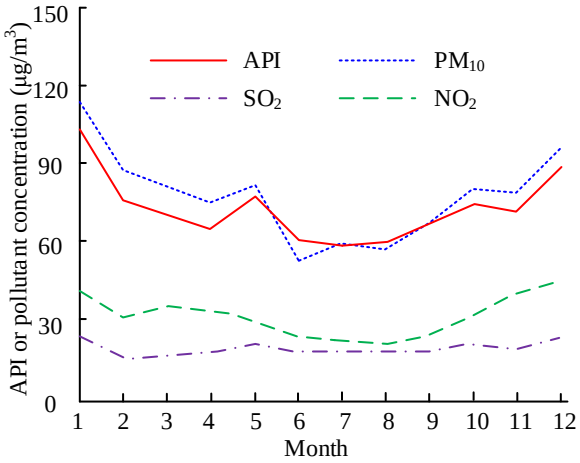

Figure 5. Monthly variation characteristics of API, PM10, SO_2, and NO_2 in 2022.

The hour-by-hour API and four types of air pollution changes on New Year's Eve and New Year's Day in the city from 2016 to 2018 were shown in Figure 6. The firecrackers during the Spring Festival were the main cause of the air pollution on this day, which was confirmed by

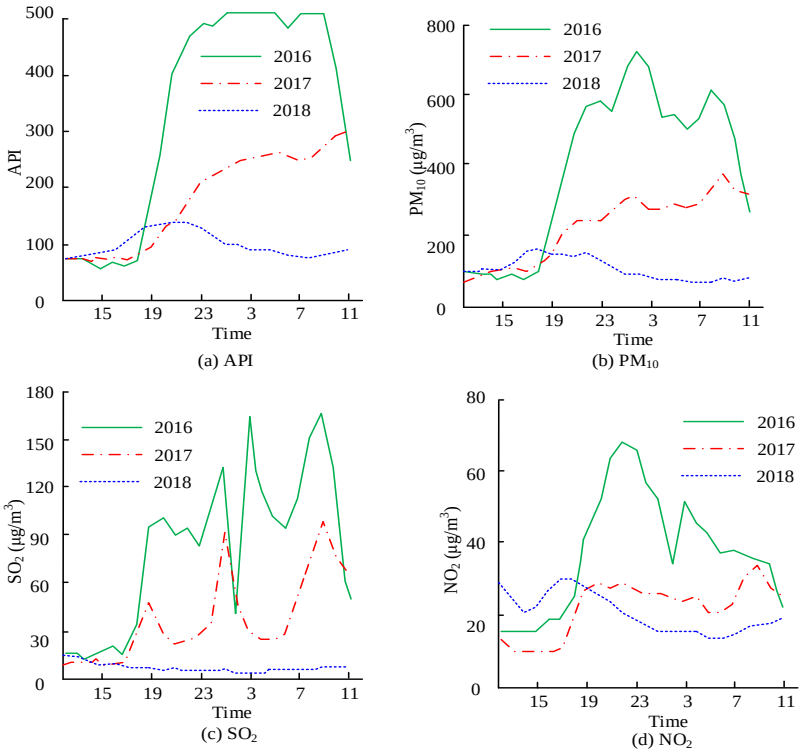

Figure 6. Hourly API and 4 types of air pollution changes on New Year's Eve and New Year's Day in the city from 2016 to 2018.

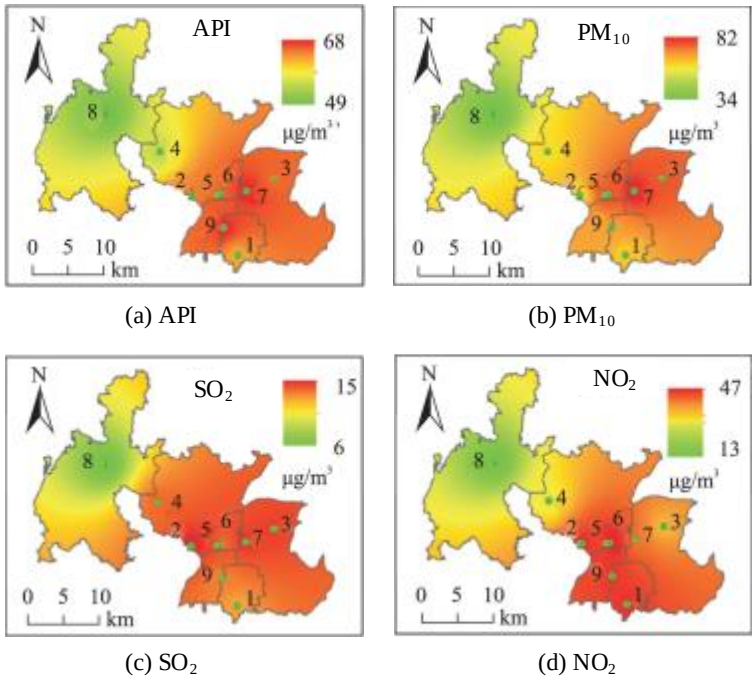

Note: Numbers 1-9 respectively indicate electromechanical school, construction engineering school, town government, forestry institute, provincial forestry company, provincial foreign Affairs Office, provincial station, martial arts school, Xianghu

Figure 7. Spatial change characteristics of pollution factors PM10, SO_2, and NO_2 at nine monitoring stations in the city in 2022.

Table 1. Model estimation results.

Variable	Model 1	Model 2	Model 3	Model 4
Ln GDP	0.0615***	-0.7028**	-	-
Ln DN	-	-	0.0208**	-0.2215
Ln Density	-0.0368***	-0.0372***	-0.0416***	-0.0412***
Ln Inno	-0.0252***	-0.0261***	-0.0187***	-0.0199**
Ln Sec	-0.0430	-0.0297	0.0156	0.0178
Ln Cons	0.0259**	-0.0104***	0.0355**	0.0322***
Ln FC	0.0025	0.0074	-0.0058	-0.0055
Ln PM10	0.8153***	0.8214***	0.7932***	0.7224***
Constant	0.6060**	4.7332***	1.2114***	2.5786***
R^2	0.9218	0.9279	0.9215	0.9247
Adjusted R2 value	0.9321	0.9346	0.9284	0.9244
F value	511.38	465.37	484.87	427.05

Notes: ***: significant result of 1%. **: significant result of 5%. *: significant result of 10%.

that the city's air quality during the Spring Festival had improved greatly, especially the concentration of PM10 and SO_2 decreased significantly since 2017 when the city's key areas were completely banned from fireworks. The spatial change characteristics of pollution factors including PM10, SO_2, and NO_2 at nine monitoring stations in the city in 2022 was shown in Figure 7. In 2022, the spatial distribution of air pollution in the city was characterized by "suburban-urban" polarization. In general, the API index in urban areas was high, especially the location of monitoring points 5, 6, and 7. Pollution factors such as PM10, SO_2, and NO_2 were consistent with the spatial distribution pattern of API values, showing heavy urban pollution and light suburban pollution.

Analysis of influencing factors of PM10, SO_2, NO_2, and API

The results of model estimation showed that population density (Density), urban technology level (Inno), and API were negatively correlated (Table 1). Regional gross domestic product (GDP) per capita had a positive impact on API. The population concentration could speed up the sharing of resources and reduce air pollution. The improvement of technical level could reduce the total amount of pollutants emitted during energy combustion, but the input of production factors would inevitably produce some air pollutants while bringing economic benefits. Although the government has strengthened environmental governance and implemented green emission reduction policies, the transformation of economic development mode is still a long-term process, and the current development mode of China's economy is still at the expense of the ecological environment. To ensure the real validity of the experimental results, this study conducted a spatial dependency test on the API value of the city. K-nearest matrix with the nearest neighbors of 4 and 6 was employed and the Moran scatter plot of the space weight matrix was obtained (Figure 8). The results showed that when the number of neighbors was different, different spatial weights demonstrated significant spatial autocorrelation, and mainly distributed in the first and third quadrants with the Moran's I values of the spatial weight matrix as 0.8301 and 0.8126, respectively, both of which passed the 1% significance level test, indicating that there was a certain spatial dependence and spatial heterogeneity in the distribution of urban air pollution. The population density coefficient was distributed in the northeast and southeast (Figure 9). With the increase of population, the environmental pollution in these cities would become more serious. There was a significant negative correlation between air pollution and population density in other regions. The distribution of urban technical level coefficient was mostly negative, mainly concentrated in the

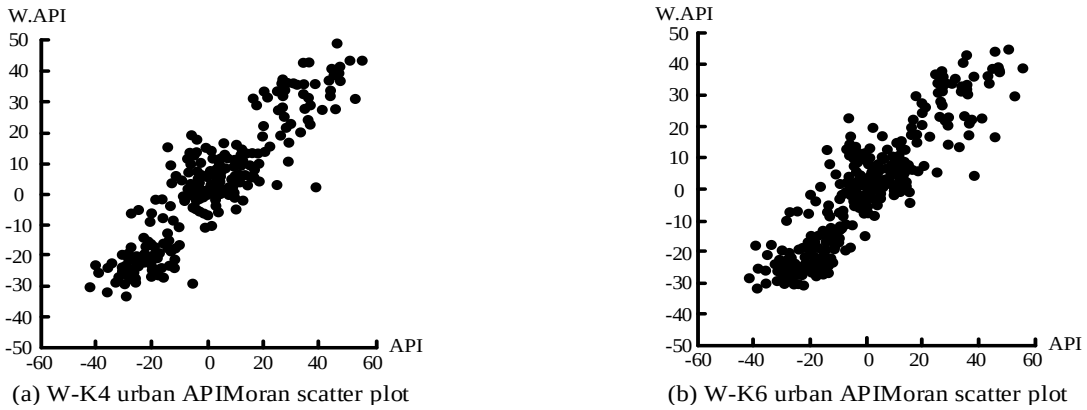

Figure 8. Moran's I scatter plot of national urban apis in 2021-2022.

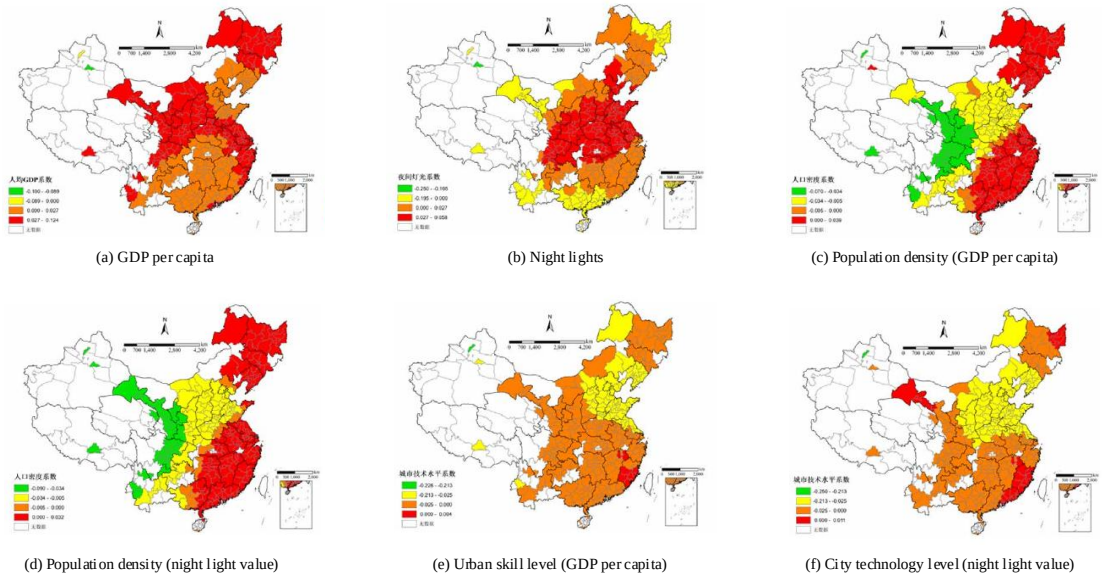

Figure 9. Spatial distribution of variable coefficients.

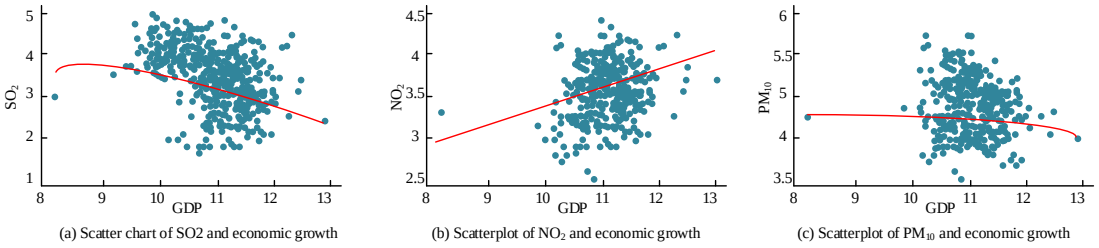

Figure 10. Scatter plot of the logarithm of real GDP per capita versus the logarithm of SO_2, NO_2, and PM10 concentrations.

Beijing-Tianjin-Hebei region, Shandong Peninsula, and other regions. The positive coefficient was concentrated in Fujian, indicating that the higher the technological content, the more serious the urban air pollution, which was due to the expansion of production scale and

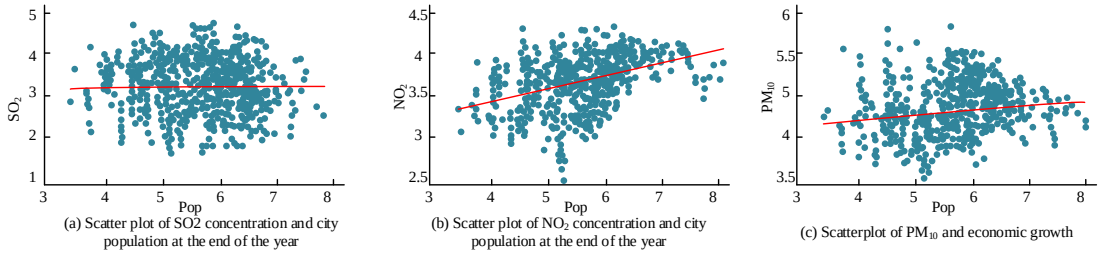

(a) Scatter plot of SO2 concentration and city population at the end of the year

(b) Scatter plot of NO_2 concentration and city population at the end of the year

(c) Scatterplot of PM_{10} and economic growth

Figure 11. The relationship between the concentrations of SO_2, NO_2, PM10 and urban population at the end of the year.

increased energy consumption with the advancement of production technology, which had exacerbated air pollution in cities. The scatter plots of the logarithms of real GDP per capita and the logarithms of SO_2, NO_2, and PM10 concentrations were shown in Figure 10. The concentration of SO2 was negatively correlated with real GDP per capita, while NO_2 concentration was positively correlated with per capita real GDP. The relationship between PM10 concentration and per capita real GDP was not obvious. The relationship between the concentrations of SO_2, NO_2, PM10 and urban population at the end of the year were shown in Figure 11. The correlation between SO_2 concentration and the population at the end of the year was not very clear, while the positive correlation between NO_2 concentration and PM10 concentration was obvious. The results showed that as the population grew, the burden on the environment would increase. Based on the scatter plot and regression curves of the real GDP per capita and the total population of the city at the end of the year with the concentrations of SO_2, NO_2, and PM10, this study provided a basic judgment on the relationship between them. With the rapid growth of the urban population, the demand for housing, household appliances, and the consumption of automobiles continue to grow, resulting in serious production and living pollution, which brings a heavy burden to the environment. When the expansion of population size exceeds a certain value, resource consumption can be saved by means of public transportation sharing rate, resource use efficiency, sharing control of pollution, and emission reduction. The benefits of the above strategies far outweigh the disadvantages of the total increase, thus reducing environmental pollution.

Conclusion

In this study, the global spatial autocorrelation method and spatial descriptive statistics method were used to explore the status of urban air pollution in China and its spatial-temporal evolution characteristics. The influencing factors were also analyzed. In the time dimension, the API index of autumn and winter decreased by 45% and 16.67%, respectively. The monthly mean value and monthly change of API showed "U" and "V" shape distributions. The concentration of PM10 and API values mostly reached more than 50 μg/m^2. The concentrations of PM10 and API showed an upward trend after 2 am and 8 pm. The "weekend effect" was obvious. In spatial dimension, the distribution of urban air pollution had certain spatial dependence and spatial heterogeneity. The pollution center gradually shrank from northwest to northeast. API monthly averages in January, June, and December of each year were analyzed and the concentration of air pollution was more obvious. In terms of influencing factors, population density and urban economic level had a negative relationship with API and main pollutants. Economic level had a positive effect on API, but it was not a completely linear relationship. There were still shortcomings in this study, which included that the selection of samples was not perfect enough, and there was a certain deviation in the measurement of the

national situation. The future research direction could start from those shortcomings.

Acknowledgement

This study was supported by the Research on the Education System of Private Colleges for the Development of Strategic Emerging Industrial Clusters in Henan Province, China.

References

1. Kurokawa J, Ohara T. 2020. Long-term historical trends in air pollutant emissions in Asia: regional emission inventory in Asia (REAS) version 3. Atmos Chem Phys. 20(21):12761-12793.
2. Qiu F, Chen Y, Tan J, Liu J, Zheng Z, Zhang X. 2020. Spatial-temporal heterogeneity of green development efficiency and its influencing factors in growing metropolitan area: a case study for the Xuzhou metropolitan area. Chinese Geogr Sci. 30: 352-365.
3. Wang ZB, Li JX, Liang LW. 2020. Spatial-temporal evolution of ozone pollution and its influencing factors in the Beijing-Tianjin-Hebei Urban Agglomeration. Environ Pollut. 256:113419.1-113419.11.
4. Jiao D, Yan L. 2022. Appraisal of urban land ecological security and analysis of influencing factors: a case study of Hefei city, China. Environ Sci Pollut R. 29(60):90803-90819.
5. Anyika L, Alisa C, Nkwoada A, Opara A, Onuoha G. 2020. Spatial-temporal study of criteria pollutants in Nigerian city. Chem Asian J. 6(3):1-13.
6. Geng G, Xiao Q, Liu S, Chen J, Zheng Y, Xue T, *et al*. 2021. Tracking air pollution in China: near real-time PM2. 5 retrievals from multisource data fusion. Environ Sci Technol. 55(17):12106-12115.
7. Gui C, Geng F, Tang J, Niu H, Teng H, Feng X, *et al*. 2022. Spatial and temporal distribution of dust pollutants from a fully mechanized mining face under the improved air-curtain system. Powder Technol. 396:467-476.
8. Kerimray A, Azbanbayev E, Kenessov B, Plotitsyn P, Alimbayeva D. 2020. Spatial temporal variations and contributing factors of air pollutants in Almaty, Kazakhstan. Aerosol Air Qual Res. 20(6):1340-1352.
9. Ma X, Longley I, Salmond J, Gao J. 2020. PyLUR: efficient software for land use regression modeling the spatial distribution of air pollutants using GDAL/OGR library in Python. Front Env Sci Eng. 14:1-14.
10. Liu X, Niu J, Yan J, Zhao C, Xu F, Zhang Y, *et al*. 2022. Surface ozone in the central plains urban agglomeration, China: spatial-temporal variations and health impacts. Pol J Environ Stud. 31(5pt.2):4767-4777.
11. Du L, Wang H, Xu H. 2020. Analysis of spatial-temporal association and factors influencing environmental pollution incidents in China. Environ Impact Assessment Review. 82:1-9.
12. Bai L, Li C, Yu C, He Z. 2021. Air pollution and health risk assessment in Northeastern China: a case study of Jilin Province. Indoor Built Environ. 30(10):1857-1874.
13. Yang Z, Qin T, Wang J, Tang J. 2021. Analysis of pollution characteristics and influencing factors of air pollutants in Beijing and Tianjin, China. J Environ Prot Ecol. 22(3):933-945.
14. Dadhich A, Goyal R, Dadhich P. 2018. Assessment of spatial-temporal variations in air quality of Jaipur city, Rajasthan, India. Egypt J Remote Sens. 21(2):173-181.
15. Zhang X, Qiu J, Qu X, Xu W, Ding H. 2021. Characteristics and influencing factors of traffic pollutant emission concentration in Shenzhen City. Sci Eng. 37(2):178-186.
16. Huang J, Zhang Y, Wang M, Wang F, Tang Z, Hao H. 2020. Spatial and temporal distribution characteristics of drought and its relationship with meteorological factors in Xinjiang in last 17 years. Acta Ecol Sin. 40(3):1077-1088.
17. Zhang D, Pei S, Duan G, Feng X, Zhang Y, Wu J. 2020. The pollution level, spatial and temporal distribution trend and risk assessment of heavy metals in Bohai Sea of China. J Coastal R. 115(SI):354-360.
18. Delgado M, Lopez A, Esteban A, Lorena L. 2022. Some findings on the spatial and temporal distribution of methane emissions in landfills. J Clean Prod. 362(15):1-8.
19. Gonzalez-Valencia R, Magana-Rodriguez F, Martinez-Cruz K. 2021. Spatial and temporal distribution of methane emissions from a covered landfill equipped with a gas recollection system. Waste Manage. 121(5):373-382.
20. Zhu Y, Chen H, Ding JP, Sun XN, Liu H, Ye JF. 2021. Distribution and influencing factors of DOM components in urban and suburban polluted rivers. Chin Environ Sci. 42(11):207-217.
21. Chang Y, Chiao H, Abimannan S, Huang Y, Tsai Y, Lin K. 2020. An LSTM-based aggregated model for air pollution forecasting. Atmos Pollut Res. 11(8):1451-1463.